Carbon fiber recycling from composite: A multimethodological approach combining pyrolysis experimental data, energy modeling, and environmental analysis

Composites: Part A 210 (2026) 110094

Contents lists available at ScienceDirect

Composites Part A

journal homepage: www.elsevier.com/locate/compositesa

Carbon fiber recycling from composite: A multimethodological approach combining pyrolysis experimental data, energy modeling, and environmental analysis

Leandro Leucci [a], Francesca Demichelis [a,*], Samir Bensaid [a], Giuseppe Mancini [b], Antonella Luciano [c], Debora Fino [a]

[a] Department of Applied Science and Technology (DISAT), Politecnico di Torino, Corso Duca degli Abruzzi 24, Turin 10129, Italy
[b] Department of Electrical, Electronic and Computer Engineering, University of Catania, Viale Andrea Doria 6, 95125, Italy
[c] Italian National Agency for the New Technologies, Energy and Sustainable Economic Development – Department for Sustainability, Casaccia Research Centre – Via Anguillarese 301, 00123, Rome, Italy

HIGHLIGHTS

- Recycling Life Cycle Assessment (LCA) for carbon-fiber-reinforced composites (CFRC)
- Experimental tests of pyrolysis yield recycled fibers with limited resin residues.
- Energy demand is the main environmental bottleneck for the pyrolysis of CFRC.
- Parametric energy model for scalable and reproducible energy evaluation for LCA.
- Inert-to-feed ratio is the most influential parameter for impact reduction.

GRAPHICAL ABSTRACT

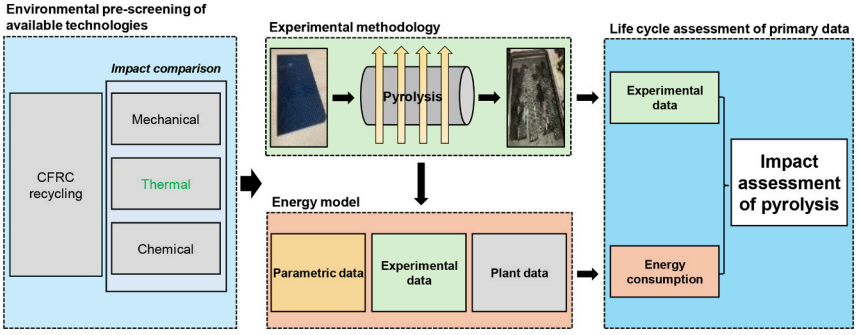

ARTICLE INFO

Keywords:
Carbon-fiber-reinforced composites
Thermal recycling
Energy model
Life cycle assessment

ABSTRACT

The study presents an integrated technical-environmental impact of carbon-fiber recycling from carbon-fiber-reinforced composites (CFRCs) through pyrolysis, combining experimental tests, parametric energy modelling, and life cycle assessment (LCA). Preliminary LCA, based on literature data comparing pyrolysis with mechanical and chemical recycling, identified energy demand as hotspot. Pyrolysis was tested at laboratory scale yielding 66.2 ± 2.4 % solid product, 12.1 ± 5.0 % oil, and 21.7 ± 2.7 % gas and 70 % of virgin mechanical properties. The obtained fibers showed high carbon content (>87 $\%_{wt}$) and limited resin residues (1–2 $\%_{wt}$). Experimental data were used to design a parametric model estimating process energy requirements under 200 kg/h. Experimental data and energy-modelling were applied in final LCA (functional unit: 1 kg CFRC waste). Sensitivity analyses, including inert gas, fuel type, thermal integration, and inert/feed ratio, showed that nitrogen and liquefied-natural-gas represent the lowest-impact configuration, while the inert/feed ratio is the highest one. Process optimization via internal energy-recovery of pyrogas was technologically unfeasible under the conditions investigated whereas the exploitation of 50 % of the oil produced as virgin phenolic compounds leads to a

* Corresponding author.
E-mail address: francesca.demichelis@polito.it (F. Demichelis).

https://doi.org/10.1016/j.compositesa.2026.110094
Received 21 May 2026; Received in revised form 27 June 2026; Accepted 9 July 2026
Available online 10 July 2026

reduction of all the impact categories. The study provides a reproducible, multi-methodological framework and identifies key levers for reducing the environmental burden of CFRC pyrolysis.

1. Introduction

Currently, carbon fibers are predominantly manufactured from polyacrylonitrile (PAN), a fossil-derived polymer that serves as the precursor for approximately 90 % of commercially available fibers [1]. The conventional production route comprises three fundamental stages: spinning, oxidation, and carbonization. Initially, PAN is processed via spinning to produce precursor filaments. These are subsequently subjected to oxidative stabilization in air at temperatures ranging from 200 to 400 °C. The process concludes with carbonization, where the stabilized fibers are heated in an inert atmosphere at temperatures up to 1000 °C to eliminate non-carbon heteroatoms and facilitate structural refinement [2]. This process is critical in terms of the cost of the precursor, which accounts for 53 % of the total process [1], and a significant environmental footprint, since polyacrylonitrile is a fossil-based polymer. In industry, carbon fibers are used in composites with a polymer matrix (epoxy resin, PP, PA6, etc.), defined as a 'fiber-reinforced polymer composite' (FRPC). Specifically, carbon fibers constitute carbon fiber reinforced composite (CFRC) with percentages between 20 and 40 %vol. These composites present high mechanical strength, high stiffness, and good corrosion resistance. In addition, they exhibit low density, making them a suitable substitute for steel in the context of weight reduction and savings in fuel consumption for the transport sector [3]. Given the wide demand for CFRC in the aerospace, automotive, and renewable energy sectors, the global market revenue is projected to rise from $ 28.2 billion to $ 48.7 billion [4]. This growth, coupled with a typical component lifespan of 15–20 years [5], necessitates effective end-of-life (EoL) strategies to prevent waste accumulation. To mitigate these challenges, research has focused on two main strategies: the development of bio-based precursors (such as lignin or cellulose) which could positively affect the overall impact in terms of consideration of biogenic origin if the carbon, and the recycling of carbon fibers from waste streams. Regarding the latter, end-of-life (EoL) processing options for CFRCs are categorized into mechanical, thermal, and chemical recycling technologies. The advantages of recycling technologies are well-documented; however, a significant gap persists in the literature regarding the transparent and reproducible assessment of their environmental impacts. Most Life Cycle Assessment (LCA) studies focus on virgin polyacrylonitrile (PAN)-based carbon fiber production, while recycling processes are typically evaluated using secondary and non-transparent industrial data. As a result, existing LCA studies on the end-of-life (EoL) treatment of composite materials exhibit three main limitations: (i) impact assessments are often based on process- or product-specific functional units, limiting generalizability; (ii) comparative analyses rely on heterogeneous inventory data from multiple sources or low-scale processes; and (iii) environmental evaluations are frequently restricted to energy use and greenhouse gas emissions, neglecting broader impact categories. Existing studies can be broadly divided into two categories: (i) analyses based on experimental processes [6,7], and (ii) comparative studies relying on literature and industrial datasets [3,8–10]. These categories share similarities with the present study in their focus on recycling assessment, but differ in terms of data quality, methodological consistency, and scalability.

In contrast to these studies, the present study integrates primary experimental data from laboratory-scale pyrolysis with a novel parametric energy model, enabling the systematic evaluation of carbon fiber composite recycling processes, according to modelling flexibility, methodological robustness, and primary data integrity. Modelling flexibility allows users to define process-specific operating conditions and derive accurate corresponding energy consumption profiles. Furthermore, the challenge of modelling unconventional material flows (such as bio-based materials) has been avoided, since the focus is on conventional fiber recycling technology, which uses petrochemical-based compounds whose material flows are generally well-documented and modeled in Ecoinvent. By shifting from secondary to primary and parameterized data, this approach enhances both the transparency and robustness of environmental impact assessments. Furthermore, it enables the identification of critical process bottlenecks and supports the development of optimization strategies aimed at reducing the environmental footprint of carbon fiber production and recycling. The main outcome is a methodology which supports moving from laboratory to industrial scale CFRC pyrolysis recycling, through direct experimental data and the definition of a scalable energetic model, together improving the consistency of the impact evaluation.

2. Materials and methods

The impact assessment of carbon fiber was performed using an integrated framework that combined complementary methodologies, following four main phases: “Phase 1” preliminary environmental analysis to evaluate the role of pyrolysis compared to mechanical and chemical treatments of CFRC waste and bottlenecks; “Phase 2” experimental tests about pyrolysis performed at the laboratory scale and design of the energetic parametric model for quantifying the energy costs of pyrolysis; “Phase 3” impact analysis of CFRC pyrolysis with primary data and sensitivity analysis with two possible scenarios; “Phase 4” evaluation of a feasibility analysis for optimization, to minimize bottlenecks in the pyrolysis process. Fig. 1 illustrates the interconnections among these approaches and highlights the specific function of each within the overall assessment process.

2.1. Preliminary environmental evaluation

The environmental evaluation was conducted according to the Life Cycle Assessment (LCA) methodology, following the ISO 14040–44:2006 standards. The LCA framework includes four main steps: goal and scope definition, life cycle inventory, impact assessment, and interpretation of results. The environmental evaluation was structured into two complementary levels, reflecting the integration between preliminary environmental assessment based on secondary data (Phase 1) and final environmental assessment on primary data (Phase 3). The preliminary environmental assessment was applied as a framework aimed at comparing the pyrolysis processing for carbon fiber reinforced composites (CFRCs) to other thermal, mechanical, and chemical treatments. Thermal treatments included pyrolysis (the core of the present study), pyrolysis/incineration, microwave pyrolysis, and fluidized bed. Mechanical treatment was concerned with grinding. Chemical treatments include strong and mild acid solvolysis, sub/supercritical solvolysis, and electrochemical treatment. The analysis is based on secondary data from the literature. Within this context, preliminary LCA served as the analytical tool providing quantitative evidence for the comparison. The goal of the preliminary environmental assessment was to compare the environmental performance of pyrolysis with mechanical and chemical recycling treatments for CFRCs, focusing on carbon fiber recycling, and identifying bottlenecks. The functional unit was defined as 1 kg of recovered carbon fiber, and the system boundaries were set from the grave to the gate. The inventory analysis was based on secondary data derived from previous studies in the literature to ensure representative inclusion of each recycling process (Table 1). The considered output was only the recovered solid (carbon fiber), while the rest (solvent and resin) was considered as emissions (“hazardous waste, unspecified treatment”). In the case of multiple studies in a single

literature work, the process data with the best fiber-resin separation result were considered. The general process scheme for all treatments and quantitative data used in the inventory is shown in the supporting information (Section 1). For each treatment, contributions to total impact were quantified in terms of energy consumption, material inputs, waste management, and transportation.

Two impact methods were applied: ReCiPe Midpoint (H) 2016 and Cumulative Energy Demand (CED, v1.12, HHV-based). These methods were chosen to provide an overview of the impacts (with ReCiPe MidPoint (H) 2016) and a focus on energy (with CED, v1.12, HHV-based). The environmental outcomes were subsequently integrated with an evaluation of technological feasibility and mechanical performance of the recovered fibers, based on literature data [5,29,30].

The combined evaluation of environmental burdens and recycled fiber quality is intended to benchmark pyrolysis against other recovery methods, highlighting its viability and critical constraints. The CFRC's system included the foreground system and background system in agreement with the study in the literature [31]. The foreground system was directly involved with reference flow management, and the background system, linked with the foreground system, included energy production, chemical supply, and avoided products. Multi-output products have been managed by expanding the boundaries of the system to include avoided primary production by recycling the materials and recovering energy from CFRCs, according to the ISO 14040 series. The adopted approach was consequential because, in this study, LCA aimed to describe how environmentally relevant flows will change in response to the selected waste treatment.

2.2. Experimental tests

To improve the quality and accuracy of mass balance data for Phase 3, an experimental campaign of pyrolysis was carried out at the laboratory scale in triplicate. The pyrolysis was conducted in a horizontal fixed-bed reactor of 1 L volume. It was carried out at 600 °C with a heating rate of 10 °C/min and a residence time of 30 min, using nitrogen as an inert gas, with a flow rate of 0.94 L/min. The operative conditions were chosen according to [32], and based on the trends detected with the thermogravimetric (TGA) analysis.

The pyrolysis was performed in triplicate and operated by treating carbon fiber composite bars (Easycomposites 2/2 twill 3 K woven carbon fiber, 3.0 mm nominal thickness) with weights for the three tests equal to 33.66 ± 3.61 g. The composition of the composite input was measured by TGA analysis, showing a fiber percentage of 59 %. At the reactor outlet, the gaseous component undergoes neutralization by quenching in an aqueous solution of NaOH (0.5 M). The gas produced was collected in a gas bag (1 L volume) at three different times (250–500 °C, 500–600 °C, 600 °C), because, by monitoring gas production, significant gas production was only observed starting at 250 °C, with a plateau around 600 °C. After cooling, the oil phase was collected by washing the reactor with acetone (99.5 %, Sigma-Aldrich) to recover the heavy oil and extracting it from the quenching solution named light oil with diethyl ether (≥99.9 %, Sigma-Aldrich). The two oil phases were separated from their respective solvents by distillation with Rotovapor (Heidolph Hei-VAP Core), with the heating bath at 50 °C and the pressure for diethyl ether and ethyl acetate solvents set at 500 mbar and 145 mbar respectively. The oil phase obtained from distillation was then collected, weighed, and the yield was calculated with Eq. (1). The same was done for the solid residue with Eq. (2), while for the gas produced, the yield was evaluated as a complement to 100.in Eq. (3)

Table 1
Summary of bibliographic references for the inventory phase of the preliminary environmental evaluation.

Treatment	*Description of process*	*References*
Mechanical	Grinding	[11]
Thermal	Pyrolysis	[10,12–14]
	Microwave pyrolysis	[15]
	Fluidized bed	[16]
Chemical	Strong acid/base solvolysis	[17,18]
	Mid acid solvolysis	[19]
	Sub/supercritical solvolysis	[20–27]
	Electrochemical	[28]

$$yield_{oil} = \frac{m_{lightoil} + m_{heavyoil}}{m_{CFRC}}(\%) \quad (1)$$

$$yield_{solid} = \frac{m_{solid}}{m_{CFRC}}(\%) \quad (2)$$

$$yield_{gas} = 100 - yield_{oil} - yield_{solid}(\%) \quad (3)$$

2.2.1. Analytical and product characterization

The chemical and physical characterization of the experimental pyrolysis products (gas, oil, and solid) was carried out to support the LCA study (of phase 3). The focus of the study was the solid product, but oil and gas were characterized to explore the possibility of their upgrading into valuable products. It was also evaluated the mechanical performance of recovered carbon fiber.

The composition of the gaseous pyrolysis products was determined using gas chromatography (SRA micro-GC). Two analytical columns were employed to enable a broad identification of compounds: the Molsieve 5A column for H_2, O_2, N_2, CO, and CH_4, and the Pora PLOT U column for CO_2, C_2H_4, C_2H_2, H_2O, C_2H_6, and C_3H_8. Gas samples were collected at three reaction-temperature intervals (250–500 °C, 500–600 °C, and 600 °C). For each interval, five replicate measurements were performed, and the mean concentration and standard deviation of each detected compound were calculated.

The chemical composition of collected oil fractions was characterized using gas chromatography coupled with mass spectrometry (GC–MS; Agilent Technologies 5975C Series GC/MSD System). Identified compounds were grouped into twelve molecular categories: phenols, polyphenols, benzenes, alcohols, ketones, esters, polyaromatics, furans, carboxylic acids, aliphatics, heterocycles, and others, to obtain

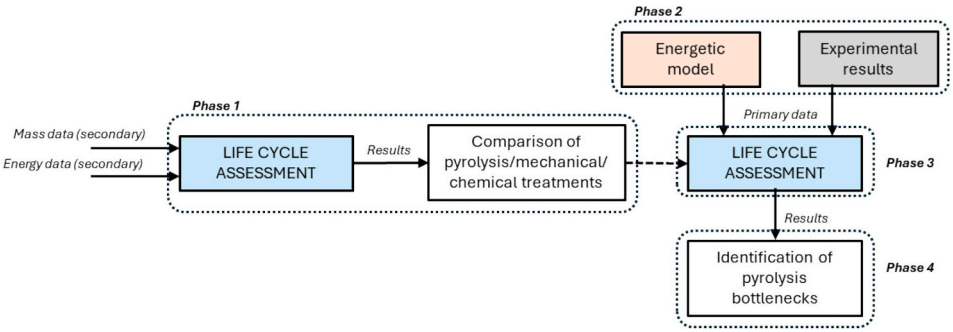

Fig. 1. Overview of the developed methodology and phases: LCA methodology (blue), energetic model (orange), experimental method (grey).

detailed chemical profiling of the oils.

Thermogravimetric analysis (TGA) was performed to quantify the inorganic fraction of the oils. Measurements were conducted up to 900 °C under an air flow of 50 mL/min and a heating rate of 10 °C/min. Elemental composition (CHNS) was determined with an Elementar Cube Vario analyzer to complement the TGA data.

The morphology and purity of the recovered carbon fibers were assessed using field-emission scanning electron microscopy (FE-SEM; Zeiss Merlin, Gemini-II column) and Fourier-transform infrared spectroscopy (FTIR). FTIR spectra were collected with a Bruker Tensor 27 spectrometer over a wavelength range of 4000–400 cm^{-1}, with a resolution of 1 cm^{-1}. Analyses were performed on the fibers both before and after washing in acetone (99.5 %, Sigma-Aldrich) to evaluate the removal of residual organic species.

Crystallinity was examined through X-ray diffraction (XRD). Diffractograms were acquired at room temperature using a Philips X'Pert PW3040 diffractometer operated at 40 kV and 40 mA, with Ni β-filtered Cu-Kα radiation ($\lambda = 1.5406 \times 10^{-1}$° m). Data were collected within a 2θ range of 10–80°, using a step size of 0.013° and a dwell time of 0.3 s per step. To assess the degree of thermochemical conversion of the composite, the H/C and O/C atomic ratios were determined for both the input material and the recovered solid residue. These data were plotted in a Van Krevelen diagram to evaluate compositional changes induced by pyrolysis.

The tensile behavior of the recovered carbon fiber tows (3 k type, 5 cm length) was evaluated through a modified tensile test procedure adapted from ASTM D4018, using ISTRON 5544. The gauge length was 25 mm, with a speed of 3 mm/min. The gripping system was pneumatic, with a pressure of 3 bars, and a methyl methacrylate adhesive was used. The average tex (g/mm) of the samples was 9.23e-04. The test was performed in triplicate.

2.3. Energetic model definition

A parametric energy model was developed to estimate the process energy demand and provide consistent energy data for Phase 3. The modeled system comprises three main sections: a thermal treatment unit, a combustion unit, and a condensation unit. The energy assessments were carried out considering an industrial-scale process, with a capacity of 200 kg/h and an initial inert/feed ratio equal to 1. The process diagram and information about the model equations can be found in supporting information (Section 2).

The energy modeling of the pyrolysis step refers to the energy balance shown in Eq. (4).

$$Q_{react} + Q_{pyr} + Q_{prod.int} = Q_{feed} + Q_{inert} + Q_{losses}(MJ) \quad (4)$$

The energy requirement for the thermal treatment step (Q_{pyr}) was determined by calculating the net process heat, obtained from the energy balance of the system, considering the sensible heat recoverable from the thermal integration of solid and gaseous products ($Q_{prod,int}$).

The term related to reaction energy (Q_{react}) represents the heat required to start the polymer decomposition within the composite matrix and was estimated using two alternative approaches according to the literature. The first was based on the difference in higher heating values (HHV) between products and reactants [33], and the second derived from a kinetic study of the thermal decomposition reaction [34].

The heat demand associated with feed and inert gas pre-heating (respectively Q_{feed} and Q_{inert}) is included as separate contributions. The inert gas type, flow rate, and inlet temperature are user-defined parameters, while the carbon fiber composite (the feed) was assumed to have a null percentage of moisture, with the latter optionally changeable as an input parameter.

Heat losses (Q_{losses}) were estimated based on natural convective heat transfer between the reactor walls, maintained at a constant temperature, and the surrounding air.

The required process heat was supplied by the combustion section, modeled as a burner producing flue gases that transfer energy to the reactor walls by convection. The model equates the heat produced by fuel combustion to the heat transferred to the system. Fuel type and combustion air conditions were defined as input parameters, influencing the corresponding energy terms. The consumption of the fuel (m_{fuel}), required to cover the process energy demand, was calculated through Eq. (5) by reporting the result as the specific energy requirement per kilogram of treated carbon fiber (E_{pyr}), considering the low heating value of the fuel used (LHV_{fuel}) and the mass of composite treated (m_{feed}).

$$E_{pyr} = \frac{m_{fuel} LHV_{fuel}}{m_{feed}} \left(\frac{MJ}{kg}\right) \quad (5)$$

Assessing the environmental impact of pyrolysis heat treatment requires a model that accounts for all relevant material and energy flows. Beyond the direct consumption of reagents and inert materials essential for the reaction, the model must also incorporate the use of auxiliary material flows, such as cooling fluids. Consequently, the established model included a potential condensation step. The thermal energy required for this step is defined as the heat that must be extracted from the post-pyrolysis gas phase to achieve complete condensation. This heat extraction was hypothesized to occur via a refrigerant fluid utilizing only its latent heat. The model allows for the selection of an appropriate refrigerant, which then dictates the necessary quantity of that refrigerant for total condensation. In this study, a simplifying assumption was made: the gas phase from the pyrolysis process was free of condensable fractions. This is based on the methodological choice that the desired oil phase is collected directly within the reactor system. A detailed summary of all input parameters required for this energy model is available in the supporting information (Section 2).

The energy model is a theoretical assessment of the energy expenditure of a process, based on energy balances, thermodynamic data, and reaction kinetics taken from scientific literature and databases. The output data was validated by comparing the data obtained with that found in the literature. During the validation phase, the energy was calculated for one kilogram of recovered fiber.

2.4. Evaluation of key properties of the composite and products

The characterization of the composite and reaction products was necessary for the evaluation of the key properties: high heating value (HHV) measured as MJ/kg, specific heat (kJ/kg °C), and enthalpy of vaporization for the oil phase (MJ/kg). These properties are fundamental for the energy evaluation of the designed model.

The high heating values were evaluated using different formulas, depending on the morphology of the referred product. Concerning the composite, the high heating value was calculated with Eq. (6), based on the experimental formula derived from Maksimuk et al [35], using data obtained from the elemental composition.

$$HHV_{CFRP} = 0.33C_{CFRP} + 1.20H_{CFRP} - 0.16O_{CFRP} \quad (6)$$

Where C, H, and O are the Carbon, Hydrogen, and Oxygen, respectively detected, for the CFRP. They were expressed in percentage. Oxygen content was measured as a complement to 100 minus ash content.

The HHVs of the solid and liquid products were evaluated using experimental formulas, applying Eq. (7) for solids [36] and Eq. (8) for the oil phase [35], taking into account the corresponding elemental compositions in percentage terms (C, H, O, S).

$$HHV_{SOLID} = 0.339C_{SOLID} + 1.256H_{SOLID} - 0.109O_{SOLID} + 0.109S_{SOLID} \quad (7)$$

$$HHV_{OIL} = 0.3517C_{OIL} + 1.1626H_{OIL} - 0.111O_{OIL} + 0.1047S_{OIL} \quad (8)$$

As regards the high heating value of the gas phase produced, the

weighted average was calculated in Eq. (9) with respect to the volumetric composition in percentage of the gas components obtained from gas chromatography analysis (X_i, i = 1,…,n).

$$HHV_{PRODGAS} = \sum_{i=1}^{n} X_i HHV_i \quad (9)$$

The specific heat for the composite, the gas phase, and the recovered solid was calculated in Eq. (10) as a weighted average of the elementary specific heats based on the composition obtained from the elemental analyzer (C, H, N, S, O). The values considered for the specific heats relating to carbon, hydrogen, nitrogen, sulfur, and oxygen were 0.71 kJ/kg °C, 14.44 kJ/kg °C, 1.04 kJ/kg °C, 0.71 kJ/kg °C, and 0.92 kJ/kg °C, respectively.

$$c_P = Cc_{P,elem,C} + Hc_{P,elem,H} + Nc_{P,elem,N} + Sc_{P,elem,S} + Oc_{P,elem,O} \quad (10)$$

The procedure used to calculate the specific heat capacity of the oil phase depends on whether gas condensation is considered in the process. In the present study, as described in Section 2.2, the produced gas was assumed to contain no condensable fraction. Consequently, the specific heat capacity of the oil phase was evaluated solely in the liquid state. In this case, the same calculation method adopted for the solid and gas phases, based on elemental composition, was applied. In contrast, when the oil phase originates from the condensation of gaseous products, the specific heat capacity should be determined by considering the individual compounds identified in the oil through gas chromatography analysis, treating these compounds in the vapor phase. The same approach was applied to the enthalpy of vaporization, which is likewise dependent on the oil composition (determined by gas chromatography analysis). This parameter should be evaluated only when the fraction of oil recovered from the condensation of the gas exiting the pyrolysis reactor is considered significant.

2.5. Environmental analysis based on primary data

The final environmental analysis was performed with LCA methodology with ISO 14040–44:2006 standards. The goal of LCA in Phase 3 was to evaluate the environmental impact of carbon fiber recovery from carbon fiber-reinforced composites (CFRC) through pyrolysis (evaluated in Phase 1), by using the energy data and experimental yield data derived from Phase 2. The step of results interpretation aimed at identifying the main contributors to the overall environmental burden and determining the parameters with the highest potential for optimization (Phase 4).

The functional unit was defined as 1 kg of treated composite waste, consistent with previous studies (Phase 1) on similar recycling processes [9,37–39]. The system boundaries were from a grave-to-gate approach, including all stages from the end-of-life of the composite to the recovery of fibers.

Input data were collected to ensure high data quality and representativeness. Experimental data were used to determine the mass balance, while a parametric energy model was employed to calculate the system's energy demand. All data used in the inventory were therefore considered primary data, derived directly from experimental and modeled results rather than from secondary databases. The investigated recycling process consisted of two main steps: a mechanical grinding stage, followed by the approach described by Howarth et al. [11], and a thermal treatment stage.

As for LCA of Phase 1, the impact assessment was performed with the ReCiPe Midpoint (H) 2016 method and the Cumulative Energy Demand (CED) method (version 1.12), the latter referenced to the higher heating value (HHV) of the energy sources involved.

The sensitivity analysis was performed by varying input parameters defined in Scenario 1 and Scenario 2.

The results of the sensitivity analysis were used to validate the LCA study and to identify and minimize the bottleneck of the process by providing an optimized analysis (Phase 4).

In Scenario 1, the inert gas was varied among nitrogen, helium, and carbon dioxide, while seven fuels (hydrogen, methane, natural gas, diesel, butane, gasoline, and liquefied natural gas) were tested. The categories with the highest quantitative impact were identified to guide subsequent analyses.

In Scenario 2, the optimal inert gas–fuel combination determined in Scenario 1 was used, and two process parameters were varied independently: (i) the extent of heat recovery from the sensible heat of the solid and gaseous products (thermal integration), and (ii) the ratio of inert gas to feed material. Thermal integration on the gaseous and solid product was conducted considering the possibility of recovering 20, 40, 60, 80, and 100 % of the thermal energy, whereas the inert-feed ratio was evaluated in the range 1–0.2 according to literature works [40–43]. The models inventory data for all the scenarios are shown in supporting information (Section 3).

In the optimization analysis, the possibility of using the gas produced as fuel within the process was evaluated, considering the higher calorific value of the gaseous product as the inert/feed parameter varies. The Wobbe index, as well as the lower and upper flammability limits (LFL and UFL) in air, were calculated. The Wobbe index was used to evaluate the interchangeability of the produced gas mixture with conventional fuels in existing burners, according to the UNI EN 437 standard, whereas the flammability limits were determined following the ASTM E681-94 method. Moreover, it was also considered the possibility of the oil product exploitation, by considering in a conservative way, that 50 % of the total oil phase from pyrolysis could be used as phenols and considering the LCA evaluation of using this product as a substitute of the same virgin quantity in the market (system expansion method).

3. Results

3.1. Preliminary environmental analysis

The preliminary environmental assessment compared the environmental performance of carbon-fiber recycling through pyrolysis with mechanical and chemical recycling processes for CFRCs. The analysis was conducted using a functional unit of 1 kg of recovered carbon fiber, and the system boundaries were defined from grave to gate. Results were examined across all midpoint impact categories included in the two assessment methods applied: ReCiPe Midpoint (H) 2016 and Cumulative Energy Demand (CED). From this comprehensive evaluation, the three most quantitatively relevant impact categories for each method were identified and selected for detailed comparison. All the impact categories result of the mechanical, thermal and chemical processes are shown in the supporting information (Section 4).

The evaluation found that the chemical process had the highest environmental impact across the three treatments, followed by the thermal process, and then the mechanical process. Considering the evaluation using the ReCiPe Midpoint (H) 2016 method, the most significant categories were identified as global warming (GW), terrestrial ecotoxicity, and human non-carcinogenic toxicity. Considering the evaluation through the CED method, the most significant categories were non-renewable fossils, non-renewable nuclear, and renewable water. Across the treatments, significant differences in impact were observed. Considering the global warming (GW), the impact range for thermal treatment (fluidized bed/ microwave pyrolysis) was 1.18 – 10.38 kg $CO_{2,\ eq}$, and for mechanical treatment (grinding) it was 0.64 kg $CO_{2,\ eq}$.

Concerning chemical treatments, it is first necessary to subdivide the overall treatments in four categories: 1) sub/super critical solvolysis using water as solvent, 2) sub/super critical solvolysis using alcohol as solvent, 3) strong acid/basic solvolysis and 4) electrochemical treatment. This implies quite different impacts within the general category of chemical recycling. Therefore, the GW was respectively 1.12 – 3.25 kg

$CO_{2,\ eq}$, 36.20 – 1833.41 kg $CO_{2,\ eq}$, 15.61– 472.94 kg $CO_{2,\ eq}$, and 21.1 kg $CO_{2,\ eq}$. The wide range of results observed for the chemical treatments can be attributed to the analyzed processes, which employed different solvent-to-composite mass ratios, with or without washing steps applied to the recovered fibers. In some cases, this could affect the estimation of solvent usage during the scale-up calculation for the LCA analysis. Fig. 2 shows the chemical, thermal, and mechanical treatments by considering the impacts calculated through ReCiPe MidPoint (H) 20,016 and CED methods.

For the ReCiPe MidPoint (H) 2016 method, Fig. 2 reports three impact categories: global warming (GW, A1), terrestrial ecotoxicity (A2), and human non-carcinogenic toxicity (A3). For both mechanical and thermal treatments, energy consumption was the dominant contributor to GW and human non-carcinogenic toxicity. Specifically, it accounts for 77.1 % and 72.6 % of the impacts for mechanical treatment, and for 87.9 % and 93.4 % for the thermal treatment, respectively.

In contrast, for terrestrial ecotoxicity (A2), the mechanical treatment showed the highest contribution from material-related processes, representing 53.5 % of the total impact. This is largely driven by transport during the composite collection phase, which alone contributes 48.8 % of the total terrestrial ecotoxicity. A similar pattern was observed for thermal treatment: although energy consumption remains the main driver, the contribution of materials and transport increases compared to the other categories, reaching 28.7 % for terrestrial ecotoxicity, 12.1 % for global warming, and 6.6 % for human non-carcinogenic toxicity.

For the chemical treatment, the different process variants are grouped due to their similar impact profiles and shared bottlenecks. In this case, materials and solvents consistently dominate the environmental impacts, contributing more than 80 % across all three categories considered.

For the CED method, Fig. 2 reports three impact categories: non-renewable fossil (B1), non-renewable nuclear (B2), and renewable water (B3). For mechanical processing, energy use contributes 75.7 % in B1 and B2 and rises to 90.1 % in B3, while even higher shares are observed for thermal treatments (94.1 %, 96.1 %, and 93.2 %, respectively). In contrast, chemical treatments show a markedly different profile, with energy accounting for less than 18 % across all categories, while the remaining 82 % represents the impact of material-related processes.

Mechanical grinding emerges as the environmentally most favorable process option, in line with its extensive industrial deployment and technological readiness level [4]. However, this advantage is offset by the poor quality of the recovered fibers, which typically retain only about 60 % of the tensile strength of virgin fibers, compared with more than 80–90 % achievable through thermal treatments [4]. Overall, pyrolysis emerges as an effective compromise between recycled fiber quality and environmental burden. Preliminary LCA results confirm that thermal treatments are environmentally preferable to chemical processes, while also emphasizing the strategic advantages of pyrolysis, such as its tolerance to heterogeneous CFRP waste streams and its high potential for automation [4]. At the same time, the predominance of energy consumption across all impact categories clearly identifies it as the main limitation of the process and the primary lever for improvement. Consequently, the following analysis focuses specifically on pyrolysis, with particular attention to strategies for reducing its energy demand and enhancing process sustainability.

3.2. Experimental method and characterization of products

The pyrolysis reaction was carried out at 600 °C with a heating rate of 10 °C/min and a residence time of 30 min, under a nitrogen atmosphere with a flow rate of 0.94 L/min. The yields were 66.2 ± 2.4 % for the solid phase, 12.1 ± 5.0 % for the oil phase (light and heavy), and 21.7 ± 2.7 %. for the gas phase. Gas composition consisted of H_2O vapor (36.1 %), CH_4 (27.1 %), H_2 (16.3 %), and the rest was composed of CO and light hydrocarbons such as ethene (C_2H_6), ethylene (C_2H_4), acetylene (C_2H_2), and propane (C_3H_8). The analysis of the oil phase composition proved the phenol-derived of the resin used in the composite. In fact, a higher presence of phenolic compounds in the oil product (> 70 %) and direct degradation of products, i.e., alcohols and benzenes (8–13

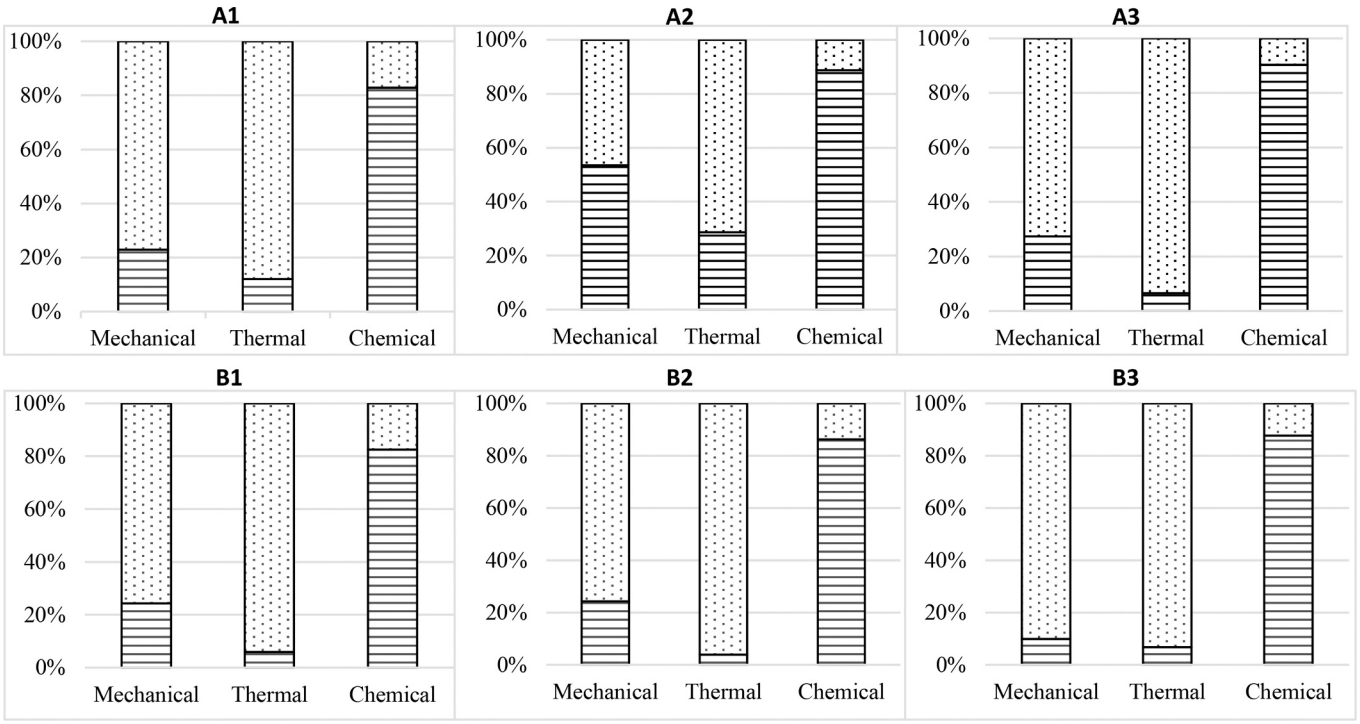

Fig. 2. Contribution of material, waste collection and transport (horizontal stripes) and energy (dotted) to overall average impact of mechanical, thermal, and chemical treatments of cfrc, for recipe midpoint (h) 2016: gw (a1), terrestrial eco-toxicity (a2), human non-carcinogenic toxicity (a3) and ced (hhv) categories: non-renewable fossil (b1), non-renewable nuclear (b2), renewable water (b3).

%) were detected. Most of the oil phase was collected directly from the reactor (approximately 90 %), while the residual part derives from the condensation of the gas phase. This allows us to consider the hypothesis of no condensation of oil from gas, an input to be specified within the energy model. The compositions measured for the gas and oil phases (supporting information, section 5) are consistent with the literature [44].

The elemental composition of the recovered solid was mainly carbon content > 87 % wt (by weight), with a hydrogen content of approximately 1 %. The latter is a consequence of the possible presence of resin residues that were not completely degraded during the pyrolysis process, which are also visible in the images obtained from FESEM microscopic analysis (Fig. 3). Residual resin traces, appearing as small fragments adhered to the fiber surface, were observed, in agreement with previous literature [56]. FTIR analysis revealed changes in the spectral regions 3200–2800 cm^{-1} and 1500–1000 cm^{-1}, associated with C–H functional groups, when comparing the solid before and after acetone washing (see supporting information, Section 6). Thermogravimetric analysis (TGA) further indicates that the residual resin content corresponds to approximately 1–2 % wt of the recovered fibers.

The structural evaluation of the solid through XRD analysis highlighted the presence of an absorption peak at an angle of $2\theta = 25.8^{\circ}$ (supporting information, section 6), relating to the graphitic structure of the carbon fiber, as expressed in the literature [45,46]. The stability of the recovered solid phase is detected by the comparison between the pristine composite and the pyrolysis-derived solid in the Van Krevelen diagram (Fig. 4). Pyrolysis induces extensive degradation of phenolic resin, leading to a marked reduction in hydrogen and oxygen contents. As a result, the recovered solid showed a pronounced shift in its O/C and H/C ratios relative to the original composite, with decreases of approximately 85 % and 97 %, respectively. In fact, pyrolytic action led to the degradation of the phenolic resin, resulting in a decrease in the hydrogen and oxygen content present in the composite, thus determining a clear difference in the recovered solid compared to the treated composite in terms of O/C and H/C (−85 % and −97 %, respectively). Characterization of the solid product was essential for populating the energy model with the requisite thermodynamic data.

Concerning the mechanical properties evaluation, due to premature damage occurring at the gripping system after the onset of tow fibrillation, the ultimate tensile strength could not be reliably determined. Therefore, the maximum load reached before the onset of tow damage was adopted. The corresponding nominal tensile stress was calculated using the equivalent cross-sectional area derived from the ratio between tow linear mass (9.23e-04 g/mm) and the fiber density (1.8 g/cm^3). The maximum measured value of peak nominal tensile stress was 1010.4 MPa. The accuracy of this value was affected by statistical filament strength distribution, load sharing and fiber alignment, making direct conversion to tensile strength unreliable. Therefore, the peak nominal tensile stress was used as a comparative parameter with virgin fiber. The parameter of virgin fiber more closely comparable with what measured

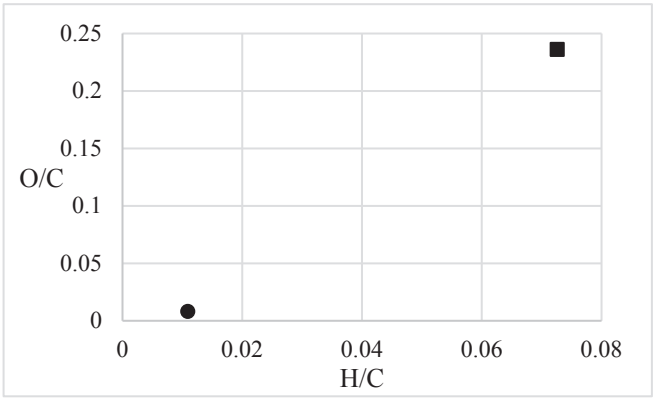

Fig. 4. Van Krevelen diagram of the comparison between composite (square) and recycled fiber (circle).

in this work was the "limit stress" introduced by Kant et al.[47], which indicates the ceasing of the typical non-linear response for single carbon fibers. This value was 1.44 GPa for the virgin fiber tow. Consequently, the comparison between the virgin fiber tow and the pyrolysis-treated tow shows a degradation of approximately 30 %.

3.3. Energetic model

The energy assessment model was developed to quantify the energy and resource consumption of the pyrolysis process, based on experimentally derived process data (paragraph 3.2). The model provides quantitative inputs for the Life Cycle Inventory (LCI) of the final LCA framework (Phase 4). All energy calculations referred to an industrial-scale configuration with a nominal processing capacity of 200 kg/h and an initial inert gas–to–feed ratio equal to 1. The model distinguished three categories of input data: experimental data, parametric data, and plant data.

Experimental data describes the thermodynamic, chemical, and physical properties of the input and output streams within the system. This category includes feed rate, reaction time, density, feed moisture content, gross calorific value, specific heat capacity, product yields, phase-change enthalpies, condensation temperatures of the oil fraction, and inlet temperatures of air and fuel. These parameters can be obtained either from direct experimental measurements (as done in the present study, paragraph 3.2) or from literature sources.

Parametric data corresponds to design and operational variables that define alternative process configurations. These inputs included the type of inert gas, the inert-to-feed ratio, the method used for reaction enthalpy calculation, the implementation of thermal integration for solid and/or gaseous products, the inclusion of gas condensation, the choice of refrigerant, plant regionality, and the fuel used to supply process heat. Parametric inputs may be either qualitative or quantitative

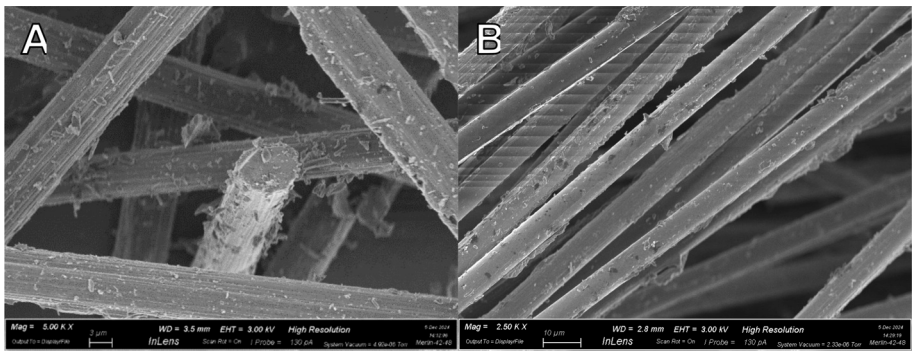

Fig. 3. FESEM images of solid recovered from pyrolysis of CFRC presenting traces of non-degraded resin: A (3 μm, 3 kV, 5 KX), B (10 μm, 3 kV, 2.5 KX).

and are constrained.

Specifically, the model consisted of:

- selection of the inert gas among helium, argon, nitrogen, and carbon dioxide.
- variation of the inert-to-feed ratio within the range 0.2–1.0, consistent with values reported in the literature (0.16–1.33) [40–43].
- variation of the fraction of sensible heat recovered from solid and/or gaseous products (0–80 %) from reaction to ambient temperature (25 °C), with the corresponding cooling water demand calculated as an output.
- selection of the heating fuel from a database of 31 conventional fuels, including solid fuels (anthracite coal, coke, semi-anthracite, semi-bituminous coal and bituminous coal), liquid fuels (tar, liquefied natural gas, ethane, propane, liquefied petroleum gas, pentane, butane, petroleum naphtha, gasoline, kerosene, gas oil, marine gas oil, diesel, paraffin, light fuel oil, heavy fuel oil, residual oil, oils vegetable, methyl ester, methyl *tert*-butyl ether, dimethyl ether, ethanol, methanol) and gas fuels (hydrogen, methane, natural gas).
- definition of plant regionality by selecting one of nine climatic zones (e.g., Mediterranean, equatorial, rainforest), which differ in ambience humidity and thus affect the energy available for pyrolysis.

Plant data represent fixed structural and design assumptions of the modeled system and are not user modifiable. These include the effective reactor volume (assumed to be 20 % of the total volume), the reactor length-to-diameter ratio (L/D = 3), and the dimensional ratio between the insulation and the reactor (external structure size/reactor diameter = 1.1).

Experimental inputs are fully quantitative and unconstrained, allowing the model to be adapted to different experimental domains. In contrast, the flexibility of parametric inputs is limited to predefined ranges and discrete options, while plant data imposes structural constraints. Consequently, the applicability of the model requires verification that the analyzed process complies with both the assumed plant configuration and the admissible parametric ranges. In this work, the yields used in the model were the same obtained by experimental test in lab-scale, keeping the reaction time at the same value (30 min) with a linear scale-up approach for the energy evaluation.

The model outputs include the specific energy demand per unit of feed, expressed both as fuel consumption (kg_{FUEL}/kg_{FEED}) and energy requirement (MJ/kg_{FEED}), as well as the cooling agent demand for condensation and thermal integration ($kg_{cooling}/kg_{FEED}$).

A schematic overview of the model structure is provided in Fig. 5.

Model validation was performed through comparison with literature data. Reported energy requirements for recycling 1 kg of carbon fiber from CFRC via pyrolysis range from 2.8 to 30 MJ [10,48,49]. Validation inputs were selected according to data type: experimental and plant data were fixed to experimentally derived and assumed values, respectively, while parametric data were systematically varied.

Gas condensation and thermal integration were excluded during validation to isolate the baseline model answer. In total, 248 validation scenarios were generated, combining two climatic regions with minimum and maximum relative humidity (Desertic and Rainforest), two inert gases with minimum and maximum specific heat (Helium and Argon), minimum and maximum inert-to-feed ratios, thirty-one different heating fuels.

The validation results confirm the robustness of the model, with approximately 88 % of the simulated cases falling within the energy range reported in the literature. The remaining cases exceed the upper bound, indicating a tendency of the model to overestimate energy demand under certain conditions. This conservative answer is consistent with the model's design to be used for environmental impact assessment. Detailed validation results are reported in the supporting information (Section 7).

3.4. Life cycle assessment: Sensitivity and scenarios optimization

The goal of this life cycle assessment (LCA) was to evaluate the environmental impacts associated with the recycling of carbon

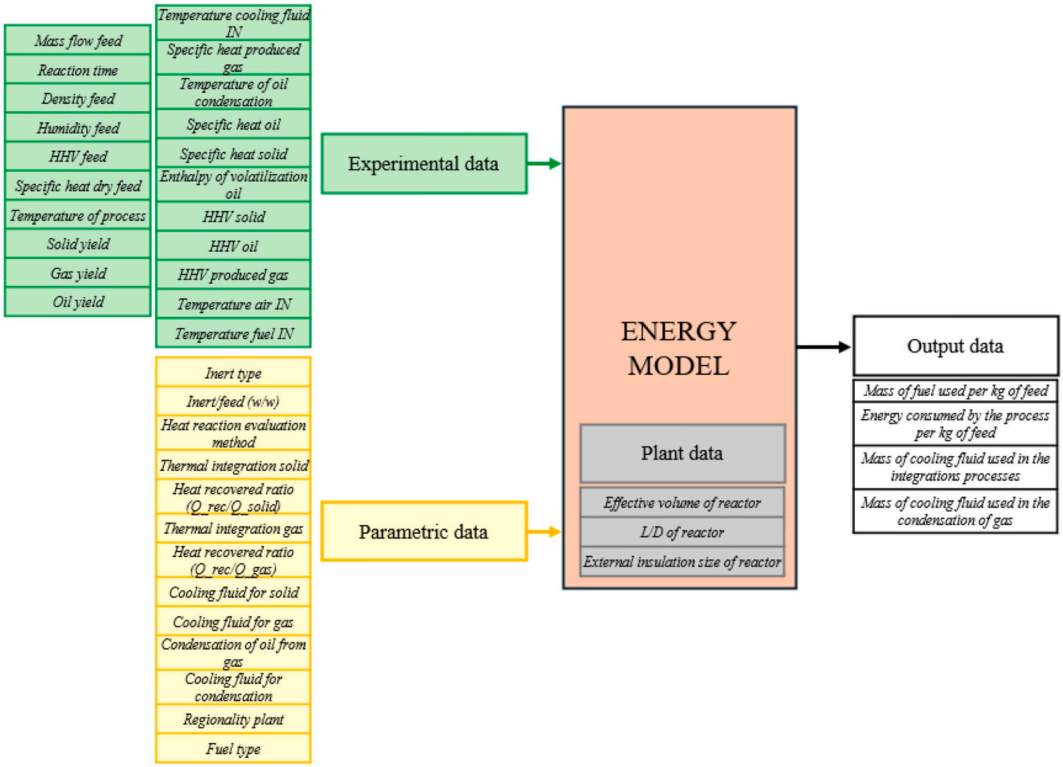

Fig. 5. Input and output data of the energetic model designed for pyrolysis (green: not constrained data; yellow: constrained data; grey: not modifiable data).

fiber–reinforced composites through pyrolysis, using experimental data and the energy model described in paragraphs 3.2 and 3.3 as primary data. The scope of the study was to identify the main contributors to the overall environmental burden of the process and to explore potential strategies for impact reduction. The functional unit was defined as 1 kg of collected composite waste. Environmental impacts were assessed using the ReCiPe Midpoint (H) 2016 and Cumulative Energy Demand (CED, HHV) methods, focusing on the most relevant impact categories.

In the LCA analyses conducted, the data relating to the material balance and characterization of the compounds resulting from the experimental process remain unchanged, while the data relating to the energy balance have been varied, as reported in paragraph 3.4.1. After this, a comparison among them has been made.

3.4.1. Sensitivity analysis

A sensitivity analysis was conducted in Phase 3 of the study through Scenarios 1 and 2 to assess the influence of key process parameters on the environmental performance of the pyrolysis process.

In Scenario 1, the effects of different inert gases and fuels were evaluated. Nitrogen, helium, and carbon dioxide were considered as inert atmospheres, while seven fuels, such as hydrogen, methane, natural gas, diesel, butane, gasoline, and liquefied natural gas (LNG), were assessed. In this scenario, the solid fraction was assumed to be the only recovered product, whereas the gaseous and oil phases were treated as emissions. Considering the average impacts across the fuels tested for each inert gas, nitrogen resulted in the lowest overall environmental impact (Table 2). Subsequently, fixing nitrogen as the inert gas, the influence of fuel type was examined, and LNG emerged as the option with the lowest impact (Table 3). Impact results for all categories are reported in the supporting information (Section 8).

In Scenario 2, further sensitivity analyses were performed starting from the optimal inert gas–fuel combination identified in Scenario 1, which was used as the baseline. Two parameters were varied independently: (i) the extent of thermal integration through the recovery of sensible heat from solid and gaseous products, and (ii) the inert gas–to–feed ratio. Thermal integration levels of 20, 40, 60, and 80 % were considered for both solid and gas phases, resulting in a total of 25 scenarios. The results indicated that global warming was the most sensitive category, with a maximum reduction of 12.5 % observed under 80 % of thermal integration compared to the non-integrated case. Other impact categories like terrestrial ecotoxicity, human non-carcinogenic toxicity, non-renewable fossil, non-renewable nuclear, renewable wind/solar/geothermal, and renewable water, showed non-significant reductions (0.01–0.04 %).

A second sensitivity analysis within Scenario 2 focused on the variation of the inert gas–to–feed ratio, ranging from 1 to 0.2, without thermal integration. This parameter variation led to substantial reductions in environmental impacts. Compared to the baseline, decreases of 13.8 %, 31.9 %, and 58.8 % were observed for global warming, terrestrial ecotoxicity, and human non-carcinogenic toxicity, respectively. Similar trends were observed for non-renewable fossil (–53.2 %), non-renewable nuclear (–67.0 %), renewable wind/solar/geothermal (–67.0 %), and renewable water (–66.6 %). Detailed results for each case are provided in the Supporting Information. The comparative influence of thermal integration and inert/feed ratio variation across impact categories is illustrated in Fig. 6, using ReCiPe Midpoint (H) 2016 and CED indicators.

3.4.2. Analysis for process optimization

Scenario 3 represents the process-optimization scenario. In Scenario 3, the potential exploitation of the thermal energy content of the gaseous product was investigated by considering all inert gas–to–feed ratios examined in the previous scenarios. The goal was to evaluate the feasibility of using the produced gas as an auxiliary fuel within the process, thereby reducing the demand for externally supplied fuels. This assessment was performed by analyzing the lower heating value (LHV) of the gas phase as a function of the amount of inert material used. The LHV ranged from 4.5 MJ/kg of gas produced at an inert/feed ratio of 1 to 13 MJ/kg at an inert/feed ratio of 0.2, corresponding to a nitrogen content in the gas phase decreasing from 82 wt% to 48 wt%, respectively. Under these conditions, the energy potentially released by combustion of the gas phase was estimated to be 5.4 MJ per kilogram of treated composite.

The interpretation of the results obtained by varying the inert agent confirmed that nitrogen is associated with lower environmental impacts compared to the other inert gases considered. From an energy standpoint, nitrogen exhibits a significantly lower specific heat than helium (1.04 and 5.19 kJ/kg·°C, respectively). Moreover, when the supply chains of inert gases are considered, nitrogen consistently shows lower impacts across all environmental categories considered in the analysis compared to carbon dioxide (complete data are reported in the supporting information, Section 8). Once nitrogen was selected as the inert gas, the influence of the fuel type was evaluated, leading to the identification of liquefied natural gas (LNG) as the fuel with the lowest overall environmental impact. This result can be attributed to the thermodynamic properties of LNG, which has one of the highest calorific values per unit mass among the fuels considered (49 MJ/kg), second only to hydrogen (120 MJ/kg). In addition, the chemical characteristics of the fuel are also relevant: assuming complete combustion, LNG releases 2.75 g of CO_2 per gram of fuel, which is the lowest value among the carbon-based fuels assessed. A comparison between LNG and hydrogen from a supply-chain perspective showed that LNG exhibits lower impacts in all categories evaluated using both the ReCiPe and CED methods (complete data are reported in the supporting information, Section 8). Consequently, based on the results of Scenario 1, the optimal inert–fuel combination was identified as nitrogen–LNG.

An analysis of the contributions of the individual input flows to the impact categories calculated using the two assessment methods allowed the identification of the main process bottlenecks for the best-performing configuration identified in Scenario 1 (see supporting information, Section 9). For the ReCiPe MidPoint (H) 2016 method, the global warming category was dominated by the pyrolysis process, which accounts for approximately 87 % of the total impact, while the inert gas supply chain represented the second-largest contributor, accounting for about 9 %.

In the case of terrestrial ecotoxicity, the largest contribution (approximately 54 %) arises from the transportation phase associated with the collection of CFRP waste, followed by the inert gas supply

Table 2
Fuel-averaged impact of pyrolysis treatment of cfrc (m: mean, sd: standard deviation) in terms of the most impactful categories in scenario 1, varying the inert agent (impact evaluated per kg of collected cfrc).

		Nitrogen	**Helium**	**Carbon dioxide**
ReCiPe MidPoint 2016 (H)		*M + SD*	*M + SD*	*M + SD*
Global warming	kg CO2 eq	2.17 ± 0.16	14.54 ± 0.35	3.59 ± 0.15
Terrestrial ecotoxicity	kg 1,4-DCB	4.27 ± 1.15	135.94 ± 2.54	11.10 ± 1.90
Human non-carcinogenic toxicity	kg 1,4-DCB	0.40 ± 0.09	4.92 ± 0.20	0.87 ± 0.09
Fossil resource scarcity	kg oil eq	0.27 ± 0.12	15.23 ± 0.27	0.34 ± 0.11
		Nitrogen	**Helium**	**Carbon dioxide**
CED (HHV)		*M + SD*	*M + SD*	*M + SD*
Non-renewable, fossil	MJ	12.24 ± 5.52	694.79 ± 12.17	15.40 ± 5.22
Non-renewable, nuclear	MJ	2.40 ± 0.08	7.84 ± 0.17	2.04 ± 0.07
Renewable, water	MJ	0.51 ± 0.03	3.11 ± 0.07	0.48 ± 0.03

Table 3
Impact of pyrolysis treatment of CFRC in nitrogen atmosphere in terms of the most impactful categories in Scenario 1, varying the fuel type (impact evaluated per kg of collected CFRC).

ReCiPe MidPoint 2016 (H)		Nitrogen Hydrogen	Methane	Natural gas	Diesel	Butane	Gasoline	LNG
Global warming	kg CO_2 eq	2.21	2.27	2.17	1.99	2.19	2.43	1.92
Terrestrial ecotoxicity	kg 1,4-DCB	5.38	2.97	5.28	3.73	5.38	4.76	2.38
Human non-carcinogenic toxicity	kg 1,4-DCB	0.41	0.58	0.38	0.32	0.46	0.34	0.29
Fossil resource scarcity	kg oil eq	0.39	0.11	0.36	0.25	0.33	0.37	0.07
CED (HHV)		**Hydrogen**	**Methane**	**Natural gas**	**Diesel**	**Butane**	**Gasoline**	**LNG**
Non-renewable, fossil	MJ	17.91	4.88	16.30	11.28	14.99	16.99	3.31
Non-renewable, nuclear	MJ	2.40	2.53	2.46	2.34	2.40	2.36	2.28
Renewable, water	MJ	0.51	0.58	0.52	0.49	0.52	0.49	0.47

(approximately 40 %). For human non-carcinogenic toxicity, the dominant contribution originated from the nitrogen supply chain (approximately 74 %), with a further 13 % attributable to the electricity supply used during the mechanical grinding pre-treatment stage.

Similarly, for fossil resource scarcity, the nitrogen supply chain was the main contributor (approximately 66 %), followed by the transportation of composite waste (approximately 21 %).

For the CED method, the non-renewable fossil category was also largely driven by the nitrogen supply chain, which accounts for 66 % of the total impact, while transportation for waste collection contributes approximately 21 %. In the case of non-renewable nuclear, the nitrogen supply chain represented the dominant contributor (approximately 84 %), followed by electricity consumption during mechanical pre-treatment (approximately 16 %). A similar trend is observed for the renewable water category, where nitrogen and electricity supply chains contributed approximately 83 % and 16 % of the total impact, respectively.

With reference to Scenario 2, the evaluation of the sensitivity analyses indicated that the quantity of inert gas used was the process parameter that had the greatest influence on the overall environmental impact, whereas the reduction in fuel consumption achieved through thermal integration has a comparatively minor effect. This finding is consistent with the results of Scenario 1, as the nitrogen supply chain represents the primary contributor to most impact categories.

An exception is observed for the global warming category, for which the influence with thermal integration was significative strong. This result is also coherent with the conclusions drawn from Scenario 1, where the pyrolysis step was identified as the main contributor to the global warming impact. It can therefore be concluded that the pyrolysis stage has a significant influence primarily on the carbon footprint of the overall treatment process, whereas for the other impact categories, the supply chains of the input flows play a more dominant role.

Concerning Scenario 3, the potential optimization based on the exploitation of the calorific value of the produced gas appears theoretically feasible. However, this energy potential must be considered as ideal, as it refers exclusively to the combustible fraction of the gaseous product. An evaluation of the lower and upper flammability limits showed that acceptable physical combustion conditions are achieved only at an inert/feed ratio of 0.2, corresponding to a lower flammability limit (LFL) of 7.7 vol% and an upper flammability limit (UFL) of 82.1 vol %. For all other inert/feed ratios, the upper flammability limit exceeds 100 vol%, indicating that the gas is highly diluted and poor in combustible components. The feasibility assessment was further completed by calculating the Wobbe index for the inert/feed ratio of 0.2, which resulted in a value of 14.2 MJ/Nm3. Since this value is below the minimum threshold of 24.8 MJ/Nm3 specified by the UNI EN 437 standard for gaseous fuels, the use of the produced gas as a fuel for thermal recovery is therefore considered unfeasible. Regarding the use of the oil phase from pyrolysis, allocating 50 % as phenols for the virgin phenol production market resulted in an overall reduction in the process's environmental impact. Looking again at the most significant impact categories for Scenario 2, the most significant reduction was recorded for the "Terrestrial ecotoxicity" and "Human non-carcinogenic toxicity" categories in the ReCiPe method, and "Non-renewable fossil" in the CED method. In all these cases, the numerical value of the impact is negative (see supporting information, section 10). In the case of GW, however, the allocation from system expansion resulted in a reduction of approximately 15 % in impact, and in the CED categories "Non-renewable, nuclear," "Renewable, wind, solar, geothermal," and "Renewable, water," reductions of approximately 23 %, 26 %, and 39 %, respectively. Consequently, utilizing a conservative percentage of the oil phase (50 % versus 80 % of measured phenolic compounds) results in a significant improvement in the overall process impact.

4. Conclusions

This study provided a comprehensive environmental assessment of carbon fiber recovery via pyrolysis, identifying key process bottlenecks and evaluating optimization strategies. Through a multi-methodological approach, made by integrating laboratory-scale tests with a novel parametric energy model, this work provided versatile primary data that addresses the current lack of transparency in recycling literature.

While the use of laboratory-scale data and idealized energy assumptions introduces inherent uncertainties for industrial scale-up, the developed model offers a robust framework for future life cycle assessments. Notably, the model's flexibility allows for the inclusion of real-world variables, such as gas condensation efficiency, regional climatic factors (e.g., air humidity for combustion), and site-specific energy mixes, enabling more granular energy evaluations.

Future research should explore the valorization of pyrolysis by-products, particularly the pyrolytic oil. In the case of phenolic resin-based composites, this fraction is rich in phenol derivatives, which serve as high-value precursors for compounds such as Nylon-6. In fact, the usage of this fraction as phenols in the industrial market seems to be promising in terms of impact evaluation, as shown in this work. Furthermore, optimizing the environmental profile of the process could involve the energetic recovery of the gas phase as a fuel substitute, the reduction of inert fractions, and the mitigation of pollutants derived from specific composite additives. This study proposes a scalable methodology to enhance the circularity of the carbon fiber industry.

CRediT authorship contribution statement

Leandro Leucci: Writing – original draft, Validation, Methodology, Investigation, Data curation. **Francesca Demichelis:** Writing – original draft, Supervision, Methodology, Data curation, Conceptualization. **Samir Bensaid:** Writing – review & editing, Visualization, Formal analysis. **Giuseppe Mancini:** Writing – review & editing, Visualization, Data curation. **Antonella Luciano:** Writing – review & editing, Visualization, Data curation. **Debora Fino:** Writing – review & editing, Project administration, Funding acquisition.

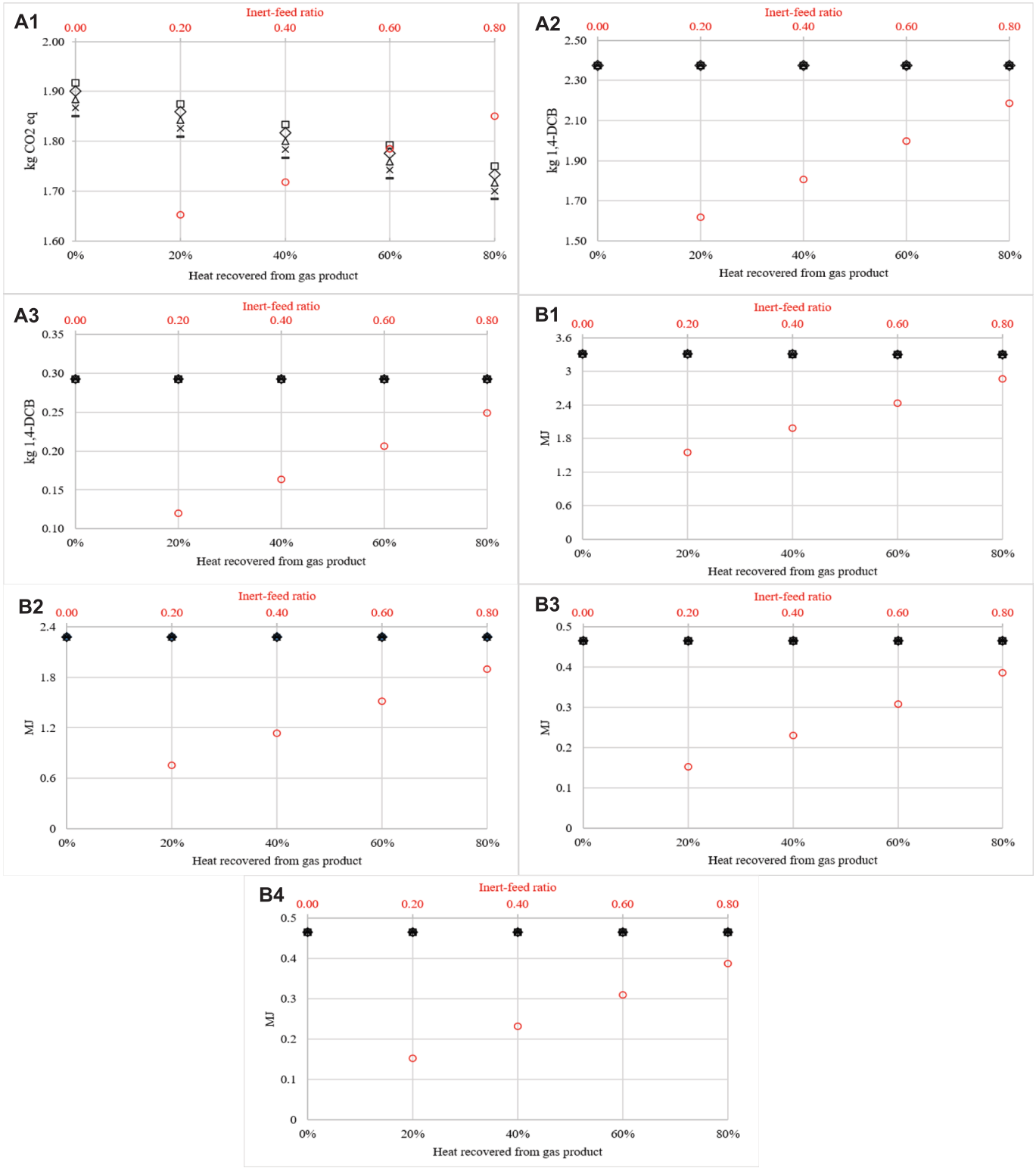

Fig. 6. Comparison of the influence of scenario 2 parameters, namely thermal integration (black markers) and inert-to-feed ratio (red markers), on the most impacted categories of ReCiPe Midpoint (H) 2016 (A1: Global Warming, A2: Terrestrial Ecotoxicity, A3: Human Non-carcinogenic Toxicity) and CED (HHV) (B1: Non-renewable Fossil, B2: Non-renewable Nuclear, B3: Renewable Wind/Solar/Geothermal, B4: Renewable Water). Different symbols denote the fraction of heat recovered from the solid product: □ (0 %), ◊ (20 %), △ (40 %), × (60 %), and – (80 %), whereas the x-axis represents the fraction of heat recovered from the gas phase.

Declaration of competing interest

The authors declare that they have no known competing financial interests or personal relationships that could have appeared to influence the work reported in this paper.

Acknowledgment

This work was supported by Stellantis Europe S.P.A. and PNRR program (MUR DM 117/2023, CUP E14D23001980004) that co-financed a PhD fellowship to the Polytechnic of Turin, Italy.

Appendix A. Supplementary data

Supplementary data to this article can be found online at https://doi.org/10.1016/j.compositesa.2026.110094.

Data availability

Data will be made available on request.

References

[1] Le ND, Varley RJ, Hummel M, Trogen M, Byrne N. A review of future directions in the development of sustainable carbon fiber from bio-based precursors. Mater Today Sustainability 2022 Dec;20:100251. https://doi.org/10.1016/j.mtsust.2022.100251.
[2] Huang X. Fabrication and Properties of Carbon Fibers. Materials 2009 Dec 16;2(4):2369–403. https://doi.org/10.3390/ma2042369.
[3] Das S. Life cycle assessment of carbon fiber-reinforced polymer composites. Int J Life Cycle Assess 2011 Mar;16(3):268–82. https://doi.org/10.1007/s11367-011-0264-z.
[4] Karuppannan Gopalraj S, Kärki T. A review on the recycling of waste carbon fibre/glass fibre-reinforced composites: fibre recovery, properties and life-cycle analysis. SN Appl Sci 2020 Mar;2(3):433. https://doi.org/10.1007/s42452-020-2195-4.
[5] Chen PY, Feng R, Xu Y, Zhu JH. Recycling and Reutilization of Waste Carbon Fiber Reinforced Plastics: Current Status and prospects. Polymers 2023 Aug 23;15(17):3508. https://doi.org/10.3390/polym15173508.
[6] Song YS, Youn JR, Gutowski TG. Life cycle energy analysis of fiber-reinforced composites. Compos A Appl Sci Manuf 2009 Aug;40(8):1257–65. https://doi.org/10.1016/j.compositesa.2009.05.020.
[7] La Rosa AD, Banatao DR, Pastine SJ, Latteri A, Cicala G. Recycling treatment of carbon fibre/epoxy composites: Materials recovery and characterization and environmental impacts through life cycle assessment. Compos B Eng 2016 Nov;104:17–25. https://doi.org/10.1016/j.compositesb.2016.08.015.
[8] Wei Y, Hadigheh SA. Cost benefit and life cycle analysis of CFRP and GFRP waste treatment methods. Constr Build Mater 2022 Sep;348:128654. https://doi.org/10.1016/j.conbuildmat.2022.128654.
[9] Vogiantzi C, Tserpes K. A Comparative Environmental and Economic Analysis of Carbon Fiber-Reinforced Polymer Recycling Processes using Life Cycle Assessment and Life Cycle Costing. J Compos Sci 2025 Jan 15;9(1):39. https://doi.org/10.3390/jcs9010039.
[10] Witik RA, Teuscher R, Michaud V, Ludwig C, Månson JAE. Carbon fibre reinforced composite waste: an environmental assessment of recycling, energy recovery and landfilling. Compos A Appl Sci Manuf 2013 Jun;49:89–99. https://doi.org/10.1016/j.compositesa.2013.02.009.
[11] Howarth J, Mareddy SSR, Mativenga PT. Energy intensity and environmental analysis of mechanical recycling of carbon fibre composite. J Clean Prod 2014 Oct;81:46–50. https://doi.org/10.1016/j.jclepro.2014.06.023.
[12] Karuppannan Gopalraj S, Deviatkin I, Horttanainen M, Kärki T. Life Cycle Assessment of a thermal Recycling Process as an Alternative to existing CFRP and GFRP Composite Wastes Management Options. Polymers 2021 Dec 17;13(24):4430. https://doi.org/10.3390/polym13244430.
[13] ELG Carbon Fibre Ltd. LCA benefits of rCF [Internet]. 2017 Mar. Available from: http://www.elgcf.com/assets/documents/ELGCF-Presentation-Composite-Recycling-LCA-March2017.pdf.
[14] Nunes AO, Viana LR, Guineheuc PM, Da Silva Moris VA, De Paiva JMF, Barna R, et al. Life cycle assessment of a steam thermolysis process to recover carbon fibers from carbon fiber-reinforced polymer waste. Int J Life Cycle Assess 2018 Sep;23(9):1825–38. https://doi.org/10.1007/s11367-017-1416-6.
[15] Akesson D, Foltynowicz Z, Christeen J, Skrifvars M. Products obtained from decomposition of glass fibre-reinforced composites using microwave pyrolysis. Polimery 2013;58(7/8):582–6. https://doi.org/10.14314/polimery.2013.582.
[16] Tyurkay A, Kirkelund GM, Lima ATM. State-of-the-art circular economy practices for end-of-life wind turbine blades for use in the construction industry. Sustainable Prod Consumption 2024 Jun;47:17–36. https://doi.org/10.1016/j.spc.2024.03.018.
[17] Liu Y, Meng L, Huang Y, Du J. Recycling of carbon/epoxy composites. J of Applied Polymer Sci 2004 Dec 5;94(5):1912–6. https://doi.org/10.1002/app.20990.
[18] Lee SH, Choi HO, Kim JS, Lee CK, Kim YK, Ju CS. Circulating flow reactor for recycling of carbon fiber from carbon fiber reinforced epoxy composite. Korean J Chem Eng 2011 Feb;28(2):449–54. https://doi.org/10.1007/s11814-010-0394-1.
[19] Xu P, Li J, Ding J. Chemical recycling of carbon fibre/epoxy composites in a mixed solution of peroxide hydrogen and N. N-dimethylformamide Composites Science and Technology 2013 Jun;82:54–9. https://doi.org/10.1016/j.compscitech.2013.04.002.
[20] Jiang G, Pickering S, Lester E, Turner T, Wong K, Warrior N. Characterisation of carbon fibres recycled from carbon fibre/epoxy resin composites using supercritical n-propanol. Compos Sci Technol 2009 Feb;69(2):192–8. https://doi.org/10.1016/j.compscitech.2008.10.007.
[21] Piñero-Hernanz R, Dodds C, Hyde J, García-Serna J, Poliakoff M, Lester E, et al. Chemical recycling of carbon fibre reinforced composites in nearcritical and supercritical water. Compos A Appl Sci Manuf 2008 Mar;39(3):454–61. https://doi.org/10.1016/j.compositesa.2008.01.001.
[22] Liu Y, Liu J, Jiang Z, Tang T. Chemical recycling of carbon fibre reinforced epoxy resin composites in subcritical water: Synergistic effect of phenol and KOH on the decomposition efficiency. Polym Degrad Stab 2012 Mar;97(3):214–20. https://doi.org/10.1016/j.polymdegradstab.2011.12.028.
[23] Piñero-Hernanz R, García-Serna J, Dodds C, Hyde J, Poliakoff M, Cocero MJ, et al. Chemical recycling of carbon fibre composites using alcohols under subcritical and supercritical conditions. J Supercrit Fluids 2008 Aug;46(1):83–92. https://doi.org/10.1016/j.supflu.2008.02.008.
[24] Okajima I, Hiramatsu M, Shimamura Y, Awaya T, Sako T. Chemical recycling of carbon fiber reinforced plastic using supercritical methanol. J Supercrit Fluids 2014 Jul;91:68–76. https://doi.org/10.1016/j.supflu.2014.04.011.
[25] Okajima I, Watanabe K, Haramiishi S, Nakamura M, Shimamura Y, Sako T. Recycling of carbon fiber reinforced plastic containing amine-cured epoxy resin using supercritical and subcritical fluids. J Supercrit Fluids 2017 Jan;119:44–51. https://doi.org/10.1016/j.supflu.2016.08.015.
[26] Bai Y, Wang Z, Feng L. Chemical recycling of carbon fibers reinforced epoxy resin composites in oxygen in supercritical water. Mater Des 2010 Feb;31(2):999–1002. https://doi.org/10.1016/j.matdes.2009.07.057.
[27] Morales Ibarra R, Sasaki M, Goto M, Quitain AT, García Montes SM, Aguilar-Garib JA. Carbon fiber recovery using water and benzyl alcohol in subcritical and supercritical conditions for chemical recycling of thermoset composite materials. J Mater Cycles Waste Manag 2015 Apr;17(2):369–79. https://doi.org/10.1007/s10163-014-0252-z.
[28] Sun H, Guo G, Memon SA, Xu W, Zhang Q, Zhu JH, et al. Recycling of carbon fibers from carbon fiber reinforced polymer using electrochemical method. Compos A Appl Sci Manuf 2015 Nov;78:10–7. https://doi.org/10.1016/j.compositesa.2015.07.015.
[29] Pimenta S, Pinho ST. Recycling carbon fibre reinforced polymers for structural applications: Technology review and market outlook. Waste Manag 2011 Feb;31(2):378–92. https://doi.org/10.1016/j.wasman.2010.09.019.
[30] Naqvi SR, Prabhakara HM, Bramer EA, Dierkes W, Akkerman R, Brem G. A critical review on recycling of end-of-life carbon fibre/glass fibre reinforced composites waste using pyrolysis towards a circular economy. Resour Conserv Recycl 2018 Sep;136:118–29. https://doi.org/10.1016/j.resconrec.2018.04.013.
[31] Clift R, Doig A, Finnveden G. The Application of Life Cycle Assessment to Integrated Solid Waste Management. Process Saf Environ Prot 2000 Jul;78(4):279–87. https://doi.org/10.1205/095758200530790.
[32] Guo L, Xu L, Ren Y, Shen Z, Fu R, Xiao H, et al. Research on a two-step pyrolysis-oxidation process of carbon fiber-reinforced epoxy resin-based composites and analysis of product properties. J Environ Chem Eng 2022 Jun;10(3):107510. https://doi.org/10.1016/j.jece.2022.107510.
[33] Kodera Y, Yamamoto T, Ishikawa E. Energy- and economic-balance estimation of pyrolysis plant for fuel-gas production from plastic waste based on bench-scale plant operations. Fuel Commun 2021 Jun;7:100016. https://doi.org/10.1016/j.jfueco.2021.100016.
[34] Dai L, Hu X, Zhou H, Liu X, Wu Y, Sun L, et al. Physicochemical, kinetic, and bond-energy analyses of the pyrolysis of carbon-fiber-reinforced polymer waste. J Anal Appl Pyrol 2025 Mar;186:106972. https://doi.org/10.1016/j.jaap.2025.106972.
[35] Maksimuk Y, Antonava Z, Krouk V, Korsakova A, Kursevich V. Prediction of higher heating value based on elemental composition for lignin and other fuels. Fuel 2020 Mar;263:116727. https://doi.org/10.1016/j.fuel.2019.116727.
[36] Mendeleev DI. Osnovy fabrichno-zavodskoj promyshlennosti [Fundamentals of manufacturing industry]. 1st ed. 1897.
[37] Poranek N, Pikoń K, Generowicz-Caba N, Mańka M, Kulczycka J, Marinis D, et al. Comparative LCA Analysis of selected Recycling Methods for Carbon Fibers and Socio-Economic Analysis. Materials 2025 Jun 5;18(11):2660. https://doi.org/10.3390/ma18112660.
[38] Yousef S, Eimontas J, Stasiulaitiene I, Zakarauskas K, Striūgas N. Recovery of energy and carbon fibre from wind turbine blades waste (carbon fibre/unsaturated polyester resin) using pyrolysis process and its life-cycle assessment. Environ Res 2024 Mar;245:118016. https://doi.org/10.1016/j.envres.2023.118016.
[39] Lefeuvre A, Garnier S, Jacquemin L, Pillain B, Sonnemann G. Anticipating in-use stocks of carbon fiber reinforced polymers and related waste flows generated by the commercial aeronautical sector until 2050. Resour Conserv Recycl 2017 Oct;125:264–72. https://doi.org/10.1016/j.resconrec.2017.06.023.
[40] Gogolev I, Perez ND, Mandviwala C, Franco RF, Johansson AC, Selander A, et al. Thermochemical recycling of mixed plastic wastes through pyrolysis and steam cracking – Assessment of centralized vs. Decentralized approaches Thermal Science and Engineering Progress 2025 Jun;62:103558. https://doi.org/10.1016/j.tsep.2025.103558.

[41] Zeller M, Netsch N, Richter F, Leibold H, Stapf D. Chemical Recycling of mixed Plastic Wastes by Pyrolysis – pilot Scale Investigations. Chem Ing Tech 2021 Nov; 93(11):1763–70. https://doi.org/10.1002/cite.202100102.
[42] Genuino HC, Van Eijk MCP, Kersten SRA, Ruiz MP. Pyrolysis of real packaging Plastic Waste Streams in a Fluidized-Bed pilot Plant. Energy Fuels 2024 Feb 1;38 (3):2188–99. https://doi.org/10.1021/acs.energyfuels.3c04114.
[43] Veses A, Martínez JD, Sanchís A, López JM, García T, García G, et al. Pyrolysis of End-Of-Life Tires: moving from a pilot Prototype to a Semi-Industrial Plant using Auger Technology. Energy Fuels 2024 Sep 5;38(17):17087–99. https://doi.org/10.1021/acs.energyfuels.4c02748.
[44] Guiles CH, Benitez Y, Morales GN, Engerer JD, Hernandez-Sanchez BA, Minton TK. Pyrolysis of Phenolic Resin Investigated by Molecular Beam Mass Spectrometry. ACS Appl Mater Interfaces 2025 Jul 9;17(27):39526–41. https://doi.org/10.1021/acsami.5c06849.
[45] Nunna S, Maghe M, Rana R, Varley RJ, Knorr DB, Sands JM, et al. Time Dependent Structure and Property Evolution in Fibres during Continuous Carbon Fibre Manufacturing. Materials 2019 Apr 1;12(7):1069. https://doi.org/10.3390/ma12071069.
[46] Galiguzov A, Malakho A, Kulakov V, Kenigfest A, Kramarenko E, Avdeev V. The Influence of Carbon Fiber Heat Treatment Temperature on Carbon-Carbon brakes Characteristics. Carbon letters 2013 Jan 31;14(1):22–6. https://doi.org/10.5714/CL.2012.14.1.022.
[47] Kant ME, Crabtree JD, Young S, Penumadu D. Concept of limit stress for the tensile behavior of carbon fiber composite tows. Compos B Eng 2020 Nov;201:108384. https://doi.org/10.1016/j.compositesb.2020.108384.
[48] Shuaib NA, Mativenga PT. Energy demand in mechanical recycling of glass fibre reinforced thermoset plastic composites. Journal of Cleaner Production 2016 May; 120:198–206. https://doi.org/10.1016/j.jclepro.2016.01.070.
[49] Khalil YF. Comparative environmental and human health evaluations of thermolysis and solvolysis recycling technologies of carbon fiber reinforced polymer waste. Waste Management 2018 Jun;76:767–78. https://doi.org/10.1016/j.wasman.2018.03.026.